proceedings

MDPI

Proceedings

Wave-Current Interactions and Infragravity Wave Propagation at a Microtidal Inlet †

Lorenzo Melito [1,*], Matteo Postacchini [1], Alex Sheremet [2], Joseph Calantoni [3], Gianluca Zitti [1], Giovanna Darvini [1] and Maurizio Brocchini [1]

[1] Department of DICEA, Università Politecnica delle Marche, 60131 Ancona, Italy; m.postacchini@univpm.it (M.P.); g.zitti@univpm.it (G.Z.); g.darvini@univpm.it (G.D.); m.brocchini@univpm.it (M.B.)

[2] Department of Civil & Coastal Engineering, Engineering School of Sustainable Infrastructure & Environment, University of Florida, Gainesville, FL 32611, USA; alex.sheremet@essie.ufl.edu

[3] Marine Geosciences Division, U.S. Naval Research Laboratory, Stennis Space Center, MS 39529, USA; code7434@nrlssc.navy.mil

* Correspondence: l.melito@pm.univpm.it; Tel.: +39-071-220-4912

† Presented at the 3rd EWaS International Conference on "Insights on the Water-Energy-Food Nexus", Lefkada Island, Greece, 27–30 June 2018.

Published: 2 August 2018

Abstract: Recent studies have shown that wave blocking occurs at river mouths with strong currents typically preventing relatively short period sea and swell waves from propagating up the river. However, observations demonstrate that lower frequency waves, so-called infragravity waves, do pass through and propagate up the river, particularly during storm events. We present observations from the Misa River estuary of infragravity wave propagation up the river during storm conditions. A model of the complex nonlinear interactions that drive infragravity waves is presented. The results are discussed in the context of an observed river mouth bar formed in the lower reach of the Misa River.

Keywords: river mouth; microtidal; wave-current interaction; infragravity waves

1. Introduction

In general, river mouths are strongly dynamic environments, where a great number of hydrological and morphological processes take place simultaneously and influence each other. The complex nonlinear interactions between waves and currents play a key role in defining the hydro-morphodynamic behavior of coastal settings like estuaries, deltas and inlets. However, the relevant features of these nonlinear interactions are still obscure and need more research to be fully understood.

A fundamental aspect of the hydrodynamics of waves and currents interacting at river mouths or tidal inlets is the phenomenon of wave blocking, in which the propagating waves are stopped by strong currents flowing in the opposite direction. As waves propagate into opposing currents, the group velocity reduces, and the wave height increases by gradual steepening. If the intensity of the outflowing current is sufficient, the relative group velocity may fall to zero and the waves get blocked. Blocking occurs when the incoming wave group velocity $C_g = -U$, where U is the (river) current velocity [1].

Wave blocking can considerably reduce the energy of sea waves penetrating the river mouth, since it favors wave steepening and energy dissipation through wave breaking. As a result, the frequency spectrum of random waves approaching a river mouth often experiences a downshift to lower frequencies. The high-frequency energy content of the wave spectrum, relative to short period,

wind-generated waves, decreases due to wave breaking and dissipation, and this energy is partially transferred to lower frequency components, i.e., to long period waves, such as infragravity waves (IG waves in the following).

The complex hydrodynamic patterns arising at the convergence of waves and riverine or tidal currents have a profound impact also on the morphological evolution of river mouths, estuaries, inlets and related environments, mainly through the generation and subsequent alteration of sedimentary bedforms. The most common sand formation occurring in the interaction zone of river jets and waves takes the form of a mouth bar, sometimes flanked by a system of parallel levees originating from the inlet corners [2]. When little to no waves are present and the flow is only due to the river jet current expanding outside the inlet, a roughly triangular mouth bar is initially generated seaward of the river mouth at a distance between zero and two channel widths from the mouth for stable jets, and at higher distances for unstable jets. The sudden drop of the sediment transport capacity of the current resulting from the jet expansion and flow deceleration favors sediment deposition. The incipient mouth bar will gradually move seaward and grow to the point of promoting significant flow deceleration and separation over it.

The intensity of the incoming waves significantly controls the evolution of the mouth bar. Traditionally, small and short waves (with significant wave height smaller than 1 m) are deemed to promote mouth bar growth in shallow mouths due to increased jet spreading, which, in turn, further lowers current velocity and transport capacity and favors sediment deposition closer to the mouth [3]. Conversely, large and energetic offshore waves suppress the formation of a mouth bar due to their enhanced erosive action and the redistributing effect of alongshore currents correlated with intense wave action [4].

Recent studies have highlighted the role of IG waves in the hydrologic and morphodynamic response of river mouths, estuaries and inlets. IG waves are ocean surface oscillations with a typical period ranging from 25–30 s to five minutes [5,6]. Although they can be directly generated by wind in some cases, most commonly IG waves are generated by sea wave groups, which occur when wave trains with slightly different wavelengths and frequencies interact. Albeit only a few centimeters in height when generated in the open sea [7], IG waves may become relevant in the nearshore, from an energetic viewpoint. Enclosed and semi-enclosed basins are particularly susceptible to propagation of IG waves; indeed, longer period waves are the most important factors for the birth of standing waves (e.g., seiches) in bays and harbours, and dominate residual sediment transport in the surf zone, promoting a significant variability in sediment suspension at time scales that are greater than those of ordinary gravity waves [8].

In small estuaries, IG waves may propagate upriver large distances from the mouth and the velocities associated with them have the potential to produce significant flows. Conceptually, the lowest reach and mouth of a river act as a low-pass filter that removes the wave energy content related to sea and swell waves, through the processes of wave blocking, steepening, breaking and direct transfer of energy to low frequency modes. Consequently, IG waves are allowed to pass through and transport their energy content farther inland. The action of penetrating IG waves over morphological processes can be relevant, as the increased sediment suspension and mobilization can potentially promote significant obstruction and closure of very shallow inlets in periods of intense wave action.

Recent work has been devoted to the analysis of the mechanisms of IG wave generation and propagation in coastal embayments. Measurements within the small estuary of the Ria de Santiuste, Spain [9] have revealed a consistent upriver propagation of waves with a narrow time periodicity of 4.3 to 4.8 min and current velocity amplitude of up to 0.1 m/s despite the strong discharging flow. The observed IG waves have been detected well into the tidal river but were generated either in the nearshore zone or in the lowest part of the estuary, where the effect of sea and swell waves was greatly reduced. Moreover, IG waves and the related currents were amplified as they progressed toward the inner parts of the river; this was presumably due to the effect of coastal edge waves that entered the estuary and produced resonance.

Field measurement campaigns conducted at the Albufeira Lagoon Inlet, a relatively shallow barrier inlet located in the wave-dominated western coast of Portugal [10], show the presence of long period oscillations in water levels within the back-barrier lagoon, due to IG waves developing in the region of the ebb inlet delta and entering the lagoon. IG wave propagation to the inner lagoon appears to be highly dependent on the tidal phase; IG waves are the most intense during the flood phase and are blocked during the ebb phase. The generation of IG waves seemed to be connected to two mechanisms. The first mechanism is related to the generation and release of bound long waves due to gravity waves breaking in the surf zone [11]; the second generation mechanism is thought to be due to the breakpoint oscillation [12], a phenomenon that acts as a low-frequency "wavemaker". Analysis of numerical simulations performed with the wave-averaged model XBeach on the Albufeira Lagoon Inlet dynamics has suggested that both mechanisms contribute to IG wave generation at the inlet, with the bound wave mechanism being more relevant outside the surf zone and the breaking point mechanism being slightly dominant over the ebb tidal delta and up to the inlet mouth.

Here we present a study of wave-current interactions and IG wave propagation at the microtidal estuary of the Misa River (Senigallia, Italy; MR hereinafter). The manuscript is structured as follows. In Section 2 the field data collected at the Misa River is briefly described. Preliminary analysis of the field data highlights the presence of IG waves at the river mouth and within the final reach of the river. A sample numerical computation of the generation of IG waves from the local wave field is also presented. In Section 3 discussion and conclusions are proposed.

2. Methods and Results

2.1. The EsCoSed Field Campaign

Between 2013 and 2014 two field sampling campaigns (part of the EsCoSed project) were conducted at the estuary of the MR and the surrounding nearshore region [13,14]. The field location shown in Figure 1 may be described as microtidal with a dissipative-to-intermediate beach. The characteristics of the field site may be assessed using the surf-scaling parameter, ϵ, the Dean parameter, Ω [15], and the relative tidal range (RTR) parameter [16],

$$\epsilon = \frac{a_b \omega^2}{g tan^2 \beta'}, \Omega = \frac{H_b}{W_s T}, \; RTR = \frac{MSTR}{H_b}, \quad (1)$$

where a_b is the breaker amplitude, H_b is the breaker height, $\omega = 2\pi/T$ is the angular frequency, T is the wave period, β is the beach slope, W_s is the sediment fall velocity and $MSTR$ is the mean spring tide range. Using as reference values those of Table 1, it is found that $\epsilon >> 20$, $5 < \Omega < 20$ and $RTR < 3$.

Figure 1. The Misa River estuary in Senigallia (Italy) depicting locations of measuring stations within the final river reach (TGdown, QR1, QR2, QR3, TGup) and in the sea (QS1, QS2, QS3).

Table 1. Reference data for characterization of the MR site.

Season	tanβ	Depth (m)	H_b (m)	T (s)	W_s (m/s)	MSTR (m)
Winter	0.01	7	3	9.5	0.011–0.032	0.5
Summer	0.01	7	1	6	0.011–0.032	0.5

The field campaigns focused on gathering observations of the meteorology, hydrodynamics, and morphodynamics, as well as collecting water and suspended sediment samples at different locations within the MR estuary and the region offshore. Prior analysis has focused on the contrast between global summertime and wintertime conditions occurring in this estuarine environment [13]. Of particular interest is the role of the wave climate on the summertime-wintertime evolution of the river. Specifically, wintertime low-flow states resembled the summertime climate, when river and sea forcing actions are both important for the hydrodynamics, resulting in a typical salt-wedge estuary. The velocity profile in the final reach of the river is characterized by a downriver flow in the upper part, due to the river discharge, and an upriver flow in the lower/nearbed part, due to the forcing of both tidal and wave actions. Conversely, high-flow states generated by storms/high precipitations were characterized by the dominance of the river discharge, hence generating a flow which is completely directed toward the sea. However, in the very final portion of the MR, the sea forcing was still important and an upriver nearbed flow existed, hence providing a convergence zone where the nearbed upriver flow became almost null (as also hypothesized in [14]). In addition, the observed winter storms were generated by northerly winds, which maintained their direction for a sufficient time and provided intense waves which easily entered the river estuary [13]. Further, while the swell component affected the estuary region, IG waves propagated upstream, hence controlling the hydro-morphodynamics of more upstream regions. On the contrary, due to reduced breaking before entering the river mouth, summertime storms produce more efficient IG waves, which propagate farther upstream, i.e., up to about 2 km, as confirmed by the summertime-campaign measurements [13].

2.2. Experimental Evidence of IG Waves at the MR

Tidal forcing propagates far upstream in the MR, even during low-flow states, as shown by the water level measurements undertaken by the Civil Protection at a number of stations along many rivers of the Marche Region. The most downstream gauge in the Misa River is that located about 1.5 km from the mouth, just upstream of the bridge called "Ponte Garibaldi". Since it is one of the most recent stations, the recordings started in 2016 and no data were collected during the wintertime EsCoSed campaign. However, the influence of tidal forcing (provided every 30 min) influences the water level at that location, while farther upstream the tide effect is negligible. The elevations at the stream gauge located near "Ponte Garibaldi" (~1.5 km from the mouth), the stream gauge located at "Bettolelle" (~9 km from the mouth) and the tide gauge located at Ancona harbor (~30 km south of Senigallia) are plotted in Figure 2. The observed elevations do not represent a hydraulic head but refer to a local vertical reference system.

Previous studies highlighted a significant penetration of IG waves into the estuary and the lower reach of the MR. Particularly, IG waves were persistent during periods when summertime storms occurred. Summertime storms have been shown to be more efficient in generating IG waves than winter storms due to lower wave heights, longer swell run, and overall reduced breaking. Figure 3 illustrates results related to a typical calm state (left panels) and to the peak of a storm (right panels) recorded in winter. The calm conditions occur on 23 January 2014 (12:00–23:00 UTC), while the stormy conditions occur on 25 January 2014 (00:00–06:00 UTC) [15]. The top panels show the flux density recorded at the offshore locations (QS2 in blue, QS1 in red). The other lines represent the flux density in the river, i.e., at the downstream tidal gauge/troll (TGdown, yellow lines), at the first (during calm state) and second (during storm) locations in the river, QR1 and QR2 (purple lines), and at the upstream tidal gauge/troll (TGup, green line). A subdivision has been made between IG and swell-sea waves. The separation frequency was calculated as 60% of the peak frequency/first harmonic. Hence, the following calculations assumed that swell and sea waves were characterized

by frequencies larger than 0.6 f_p, while IG waves fall in the frequency range (1/300–0.6 f_p) Hz. The variance flux (bottom panels) has been estimated for each condition by integrating the flux density over the frequency, with the aim to investigate its spatial evolution. The partitioning leads to swell-sea waves always dominating in the sea, while the IG waves seem to increase their energy in the river and overcome the swell-sea-derived energy, especially during storms (bottom right).

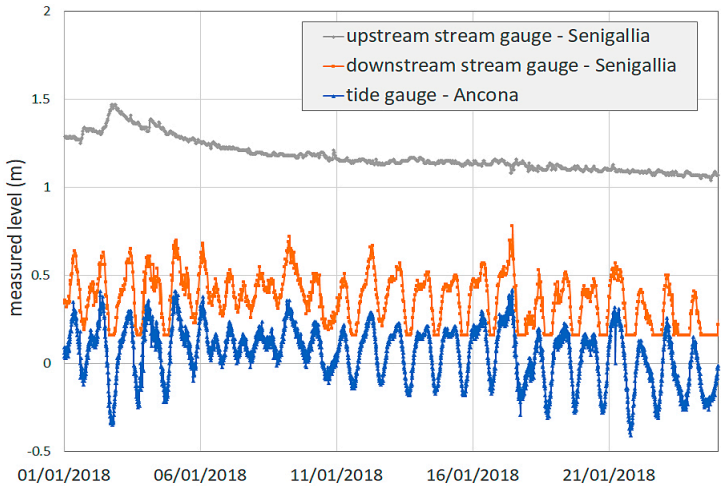

Figure 2. Water elevation measured by stream gauges located at "Bettolelle" (~9 km from the mouth, gray) and near "Ponte Garibaldi" (~1.5 km from the mouth, orange), both referring to a local reference system. Comparison is made with observations from the tide gauge located at Ancona harbor (blue).

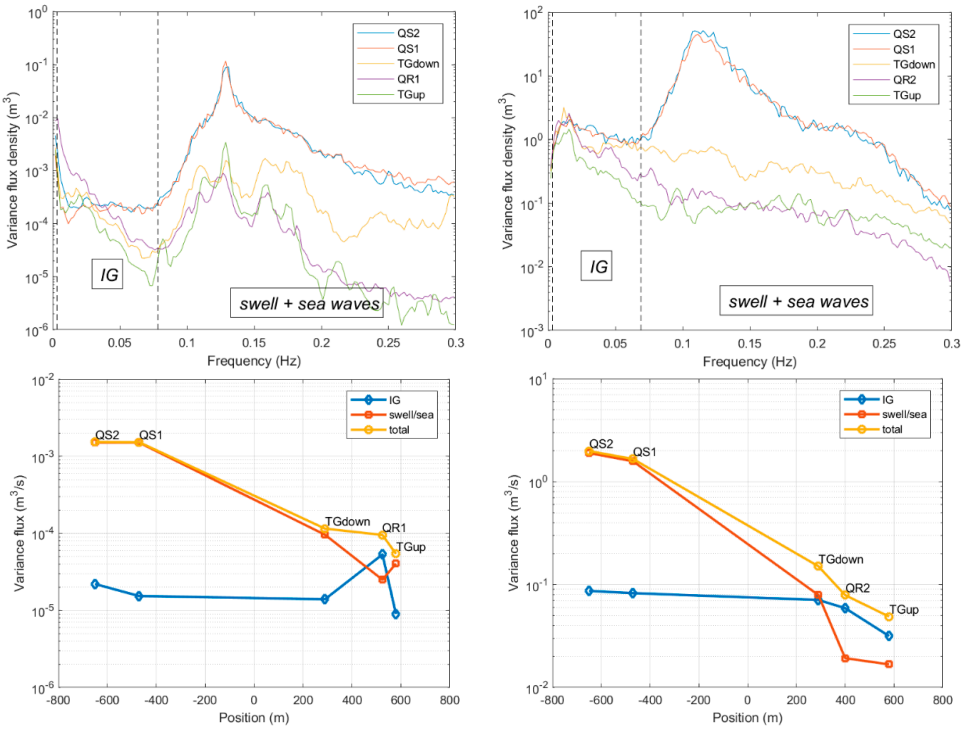

Figure 3. Spectral analysis shows energy flux (**top**) and band energy flux (**bottom**) at different locations in the Misa River mouth and nearshore during both calm (**left**) and storm (**right**) conditions.

Signals for locations QS1 and QS2 (top panels) significantly overlap and show a peak in correspondence of the typical waves of the Adriatic Sea, characterized by peak periods T_p = (7–9) s. During the calm period, the flux density distribution that characterizes the river gauges (top left) was similar to those of the offshore locations, with almost all peak periods referring to swell-sea waves, while the stormy state (top right) was characterized by lower f_p and larger T_p in the river. Hence, IG waves dominated and propagated more easily upriver during storms rather than during calms,

which was also confirmed by the variance flux (bottom panels), where the largest energy was mainly provided by the swell-sea, with the IG waves playing a minor role at the offshore locations. In the river, the IG waves dominated only at location QR1 during calm conditions (bottom left), while their magnitude is significantly larger during storm conditions (bottom right).

The significant wave height, H_{m0}, has been estimated at all observing locations, to investigate their spatial evolution and decay. Figure 4 illustrates that the significant wave height significantly decayed, with the swell-sea waves providing the largest contribution offshore in both cases. The IG contribution became much more important in the upstream portions of the river, in agreement with the band energy flux shown in Figure 3. Storms (right panel) provided significant dissipation due to breaking, as the total wave height at the gauge closest to the mouth (TGdown) was 32% of that measured at the offshore location (QS2). On the contrary, the IG wave height (in blue) slightly increased while moving toward the river, where it represented about (75–80)% of the total wave height (in yellow).

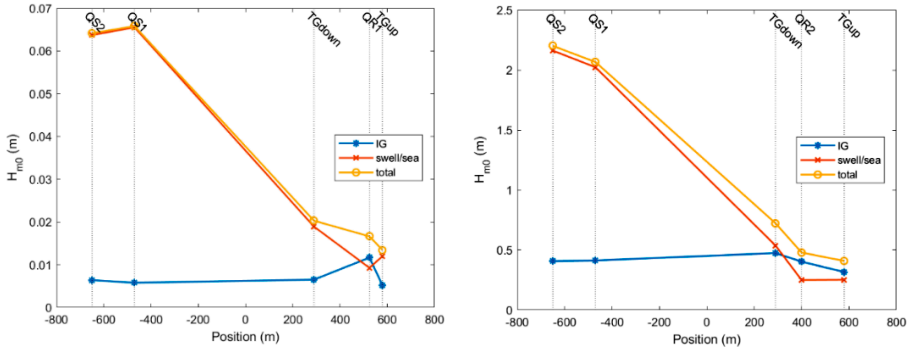

Figure 4. Evolution of the significant wave height, H_{m0}, during both calm (**left**) and storm (**right**) conditions is shown with the total wave height (o) and the contributions from IG (*) and swell-sea (x).

2.3. TRIADS Sample Computation of the Generation of IG from the Local Wave Field

TRIADS is a phase-resolving triad interaction formulation for directional wave propagation over nearly cylindrical (alongshore uniform bathymetries). The model is an extension of unidirectional models proposed for the first time for shallow water [17] and later recast [18] in a uniformly-valid formulation for arbitrary depth using the mild-slope equation. The current numerical implementation of the TRIADS model [19] has been widely described and applied [20]. In the simulation results (Figure 5), the beach was assumed to be cylindrical (laterally uniform) and mildly sloping in the cross-shore direction. Such results represent averages over 100 realizations of the wave field measured at the most offshore location (QS3). The initial condition for each realization was constructed by converting the estimated directional spectral density to amplitude spectrum and associating it to a set of random phases uniformly distributed between $-\pi$ and π.

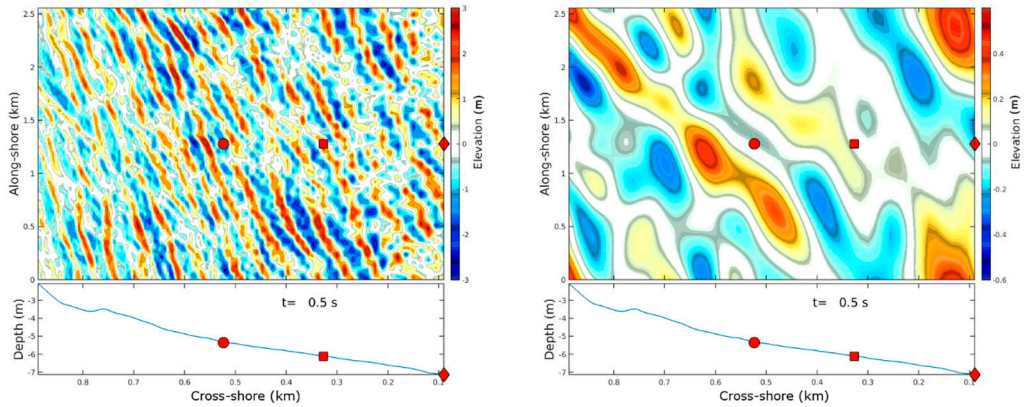

Figure 5. An example of a realization of the nonlinear wave shoaling simulated using TRIADS on the beach fronting the Misa river mouth, showing the sea and swell wave field (**left panel**) associated with the IG field (**right panel**).

3. Discussion and Conclusions

As demonstrated by field observations and numerical simulations, wave propagation from offshore to the river mouth provided an energy redistribution throughout wave frequencies, with dissipation of high-frequency components due to breaking. In the specific case analyzed here, the propagation of IG waves inside the Misa river was of importance for both the hydrodynamics and the morphological processes that develop at the estuary and farther upstream. Both calm and storm conditions were characterized by frequency distributions with peak periods around (7–9) s in the coastal region, but whereas the sea and swell waves are seen to dominate offshore in both conditions, IG waves increase their relative role within the river; this is especially true during stormy states. Storm-related energy spectra within the river are also shifted towards lower frequencies, suggesting that IG waves propagate more easily into the river mouth during storms. In addition, waves experience a strong dissipation due to breaking (especially during storms) and a relevant height reduction while approaching and entering the river mouth: while the swell wave height decreases from the offshore to the inner reach of the river, in agreement with the decrease of the total wave energy, the IG contribution to water height slightly increases to the point of becoming dominant inside the river, where it makes up to 80% of the total wave height. Computations by means of the TRIADS model further confirm the presence of an IG field associated with sea and swell waves in the nearshore region in front of the river mouth.

Given the observations of IG waves in the final river reach, it seems necessary to further investigate the role of such long-wave modes on the local sediment transport and morphodynamics. Particularly, the role that IG waves have on the evolution of internal mouth bars is illustrated by the SGS videomonitoring station active at the Misa River mouth [21] (Figure 6). Although most of the sediment that makes up the mouth bar comes from sediments transport downriver (from clayey silts to gravel), IG and tidal waves are seen to influence the remolding and slow migration of the bar.

Figure 6. Illustration of sedimentary deposition creating an internal mouth bar at the final reach of the Misa River. The lower panel gives the tidal level.

Acknowledgments: The financial support from the Office of Naval Research Global (UK) NICOP EsCoSed Project (Research Grant N62909-13-1-N020) and MORSE Project (Research Grant N62909-17-1-2148) is acknowledged. Joseph Calantoni was supported under base funding to the U.S. Naval Research Laboratory from the Office of Naval Research.

References

1. Chawla, A.; Kirby, J.T. Monochromatic and random wave breaking at blocking points. *J. Geophys. Res. Oceans* **2002**, *107*, 4-1–4-19.
2. Fagherazzi, S.; Edmonds, D.A.; Nardin, W.; Leonardi, N.; Canestrelli, A.; Falcini, F.; Jerolmack, D.J.; Mariotti, G.; Rowland, J.C.; Slingerland, R.L. Dynamics of river mouth deposits. *Rev. Geophys.* **2015**, *53*, 642–672.
3. Nardin, W.; Mariotti, G.; Edmonds, D.A.; Guercio, R.; Fagherazzi, S. Growth of river mouth bars in sheltered bays in the presence of frontal waves. *J. Geophys. Res. Earth Surf.* **2013**, *118*, 872–886.
4. Jerolmack, D.J.; Swenson, J.B. Scaling relationships and evolution of distributary networks on wave-influenced deltas. *Geophys. Res. Lett.* **2007**, *34*, doi:10.1029/2007GL031823.
5. Davidson-Arnott, R. *An Introduction to Coastal Processes and Geomorphology*; Cambridge University Press: Cambridge, UK, 2009.
6. Munk, W.H. Origin and generation of waves. In Proceedings of the First Conference on Coastal Engineering, Long Beach, CA, USA, October 1950.
7. Aucan, J.; Ardhuin, F. Infragravity waves in the deep ocean: An upward revision. *Geophys. Res. Lett.* **2013** *40*, 3435–3439.
8. Aagaard, T.; Hughes, M. Sediment transport. In *Reference Module in Earth Systems and Environmental Sciences*; Elsevier Science: New York, NY, USA, 2013; pp. 74–105.
9. Uncles, R.J.; Stephens, J.A.; Harris, C. Infragravity currents in a small ría: Estuary-amplified coastal edge waves? *Estuar. Coast. Shelf Sci.* **2014**, *150*, 242–251.
10. Bertin, X.; Olabarrieta, M. Relevance of infragravity waves in a wave-dominated inlet. *J. Geophys. Res. Oceans* **2016**, *121*, 5418–5435.
11. Longuet-Higgins, M.S.; Stewart, R.W. Radiation stresses in water waves; a physical discussion, with applications. *Deep Sea Res. Oceanogr. Abstr.* **1964**, *11*, 529–562.
12. Symonds, G.; Huntley, D.A.; Bowen, A.J. Two-dimensional surf beat: Long wave generation by a time-varying breakpoint. *J. Geophys. Res. Oceans* **1982**, *87*, 492–498.
13. Brocchini, M.; Calantoni, J.; Postacchini, M.; Sheremet, A.; Staples, T.; Smith, J.; Reed, A.H.; Braithwaite, E.F., III; Lorenzoni, C.; Russo, A.; et al. Comparison between the wintertime and summertime dynamics of the Misa River estuary. *Mar. Geol.* **2017**, *385*, 27–40.
14. Brocchini, M.; Calantoni, J.; Reed, A.H.; Postacchini, M.; Lorenzoni, C.; Russo, A.; Mancinelli, A.; Corvaro, S.; Moriconi, G.; Soldini, L. Summertime conditions of a muddy estuarine environment: The EsCoSed project contribution. *Water Sci. Technol.* **2015**, *71*, 1451–1457.
15. Wright, L.D.; Short, A.D. Morphodynamic variability of surf zones and beaches: A synthesis. *Mar. Geol.* **1984**, *56*, 93–118.
16. Masselink, G.; Short, A.D. The effect of tide range on beach morphodynamics and morphology: A conceptual beach model. *J. Coast. Res.* **1993**, *9*, 785–800.
17. Freilich, M.H.; Guza, R.T. Nonlinear effects of shoaling surface gravity waves. *Philos. Trans. R. Soc. Lond. A* **1983**, *311*, 1–41.
18. Agnon, Y.; Sheremet, A.; Gonsalves, J.; Stiassnie, M. A unidirectional model for shoaling gravity waves. *Coast. Eng.* **1993**, *20*, 29–58.
19. Davis, J.R.; Sheremet, A.; Tian, M.; Saxena, S. A numerical implementation of a nonlinear mild slope model for shoaling directional waves. *J. Mar. Sci. Eng.* **2014**, *2*, 140–158.
20. Sheremet, A.; Davis, J.R.; Tian, M.; Hanson, J.L.; Hathaway, K.K. TRIADS: A phase resolving model for nonlinear shoaling of directional waves. *Ocean Model.* **2016**, *99*, 60–74.
21. Perugini, E.; Soldini, L.; Palmsten, M.L.; Calantoni, J.; Brocchini, M. A new video monitoring station along the Adriatic coast. In Proceedings of the Convegno Nazionale di Idraulica e Costruzioni Idrauliche, Ancona, Italy, 12–14 September 2018.